Internal rotation and Stark effect in CH_3SiD_3

Irving Ozier
Department of Physics and Astronomy, University of British Columbia, 6224 Agricultural Road, Vancouver, British Columbia V6T 1Z1, Canada

W. Leo Meerts
Department of Molecular and Laser Physics, University of Nijmegen, P.O. Box 9010, 6500 GL Nijmegen, The Netherlands

(Received 8 April 1998; accepted 19 June 1998)

The avoided-crossing molecular-beam method has been applied to CH_3SiD_3 in the ground torsional state ($v_6=0$). Three ''rotational'' anticrossings have been measured corresponding to normally forbidden transitions in which both the rotational and leading torsional energy terms change. Each torsional sublevel with $(J=4,k=\mp 1)$ and given torsion–rotation symmetry Γ undergoes an avoided crossing with its counterpart with $(J=3,k=\pm 2)$ and the same Γ. Four ''barrier'' anticrossings have been measured corresponding again to normally forbidden transitions, but in which only the torsional energy changes. These transitions are $(J\leftrightarrow J)$, $(k=\pm 1\leftrightarrow\mp 1)$, and $(\Gamma=E_3\leftrightarrow E_2,E_1)$ for $J=1$ and 2. From these seven zero-field splittings and nine existing R-branch microwave frequencies for $v_6\leqslant 2$, nine torsion–rotation parameters have been determined including the effective rotational constant $A^{\rm eff}=34\,192.04(11)$ MHz and the effective height of the barrier to internal rotation $V_3^{\rm eff}=585.08(5)\ {\rm cm}^{-1}$. For each anticrossing studied, an estimate has been made of the contribution $\delta\nu_{\rm hyp}$ to the zero-field splitting from the nuclear hyperfine interactions. For CH_3SiH_3, CH_3CD_3, and CH_3SiF_3, barrier anticrossings have been previously investigated. For each of these anticrossings, estimates of $\delta\nu_{\rm hyp}$ are made here as well. For all cases studied (including those for CH_3SiD_3), it is found that $|\delta\nu_{\rm hyp}|\lesssim 5$ kHz. For CH_3SiD_3, by using conventional electric-resonance molecular-beam methods, the electric dipole moment has been determined to an accuracy of ~ 55 ppm for each of the rotational states $(J,k)=(1,\pm 1)$, $(2,\pm 1)$, and $(3,\pm 2)$.
 [S0021-9606(98)01236-7]

I. INTRODUCTION

In the study of internal rotation,[1,2] the physical interpretation of the effective parameters that characterize the Hamiltonian and electric dipole operators is complicated primarily by two effects. First, there is a series of redundancies that prevents the separation of many of these parameters into the individual contributions that arise from different physical mechanisms.[3–6] Second, the coupling between different vibrational modes often involves levels in which the molecule is undergoing large amplitude torsional motion.[7,8] The form of these coupling operators has not been investigated extensively enough to establish how the higher vibrational states contribute to the effective parameters for the ground vibrational state when the coupling is removed by the usual contact transformation.

The physical interpretation of these effective parameters is simplest for a symmetric top with one torsional degree of freedom. The prototype for such molecules has come to be CH_3SiH_3. An extensive series of high-resolution spectroscopic studies has been carried out over the last two decades; see Ref. 9 and the references cited therein. To discuss the part of this work that is directly relevant here, we can confine attention to the ground vibrational state. The torsional levels are distinguished by $v_6=0,1,2,\ldots$. For each rotational state (J,k), there are three torsional sublevels labeled by the index $\sigma=0,+1,-1$. Note that k can be positive or negative; see Ref. 10. In the early part of the CH_3SiH_3 series of investigations, the pivotal step was the measurement in the ground torsional state of the σ-splittings for various (J,k) by the molecular-beam avoided-crossing method.[11] This particular technique was developed[12] for such purposes because the dipole selection rules preclude the use of more conventional forms of spectroscopy. A precision determination of the electric dipole moment μ was carried out because μ is required to convert each crossing field ξ_c measured to the corresponding zero-field energy difference (or ''frequency'' as it is often referred to).

One method of obtaining further insight into the physical meaning of the effective parameters is to study their isotopic dependence. The purpose of the current work is to begin a study of this dependence in methyl silane, initiating a series of investigations on CH_3SiD_3 similar to that on the parent isotopomer CH_3SiH_3.

The present work on CH_3SiD_3 parallels that in Refs. 13 and 11 on CH_3SiH_3. Here the dipole moment has been measured by conventional molecular-beam electric-resonance techniques to an absolute accuracy of ~ 55 ppm for each of the rotational states $(J,k)=(1,\pm 1)$, $(2,\pm 1)$, and $(3,\pm 2)$. For $J=1$, two anticrossings were measured corresponding to the normally forbidden zero-field transitions $(J=1,k=\pm 1,\sigma=\mp 1)\leftarrow(J=1,k=\mp 1,\sigma=\mp 1)$ and $(J=1,k=\pm 1,\sigma=\mp 1)\leftarrow(J=1,k=\mp 1,\sigma=0)$; see Ref. 14. These are called ''barrier'' anticrossings because the energy

differences arise entirely from the torsional terms in the Hamiltonian (except for small corrections). For $J=2$, the corresponding pair of anticrossings was measured as well. Three anticrossings in which J changes by unity were observed corresponding to the normally forbidden zero-field transitions $(J=4,k=\mp 1,\sigma)\leftarrow(J=3,k=\pm 2,\sigma)$ for $\sigma=0$, $\pm 1,\mp 1$. These are called ''rotational'' anticrossings because the energy differences contain a contribution from the rotational Hamiltonian.

An investigation of the microwave absorption spectrum[15] led to the determination of pure rotational frequencies $\nu_R(v_6,J,k,\sigma)$ obeying the normal dipole selection rules $\Delta J=\pm 1$, $\Delta k=0$, and $\Delta\sigma=0$. The transitions measured were $(J,k)=(1,0)\leftarrow(0,0)$ and $(2,\pm 1)\leftarrow(1,\pm 1)$ for $v_6\leqslant 4$, but there were some difficulties for $v_6=3$ and 4. The σ-splitting for given (v_6,J,k) was resolved only for $v_6\geqslant 2$. In the absence of perturbations from excited vibrational states, this σ-splitting is determined primarily by the σ-dependence of the effective B-value (and is insensitive to the leading terms in the torsional Hamiltonian).

From the analysis of the seven molecular-beam zero-field frequencies and nine pure rotational frequencies with $v_6\leqslant 2$, values were obtained for nine parameters in the torsion–rotation Hamiltonian including effective values for the A-rotational constant and the barrier height V_3. These results are compared with their counterparts for CH_3SiH_3 obtained in Ref. 11 from the analysis of a similar body of data. The anticrossing data presented here for CH_3SiD_3 will be very useful in the analysis of high-resolution infrared bands currently under study.[16]

In the Appendix, the question is reexamined as to whether the nuclear hyperfine interactions contribute in lowest order to the zero-field frequencies determined from the barrier anticrossings. Contrary to arguments presented earlier,[11] it is shown here that this contribution can be the order of the diagonal matrix elements of the hyperfine Hamiltonian. For CH_3SiD_3, an estimate has been made of the nuclear hyperfine contribution. Adjustments were then made to the errors assigned to the zero-field frequencies used in the torsion–rotation analysis. Similarly, estimates of the hyperfine contributions have been made for each of the molecules for which barrier anticrossings have previously been measured, namely CH_3SiH_3,[11] CH_3SiF_3,[17] and CH_3CD_3.[18] In all cases, the hyperfine contribution has been estimated to be $\lesssim 5$ kHz in magnitude. The hyperfine contributions to the rotational anticrossing frequencies measured here in CH_3SiD_3 are shown to average to zero to first order.

II. THEORETICAL BACKGROUND

A. Torsion–rotation energy

For a symmetric rotor with a single torsional degree of freedom, the torsion–rotation Hamiltonian $\tilde{H}_g$ appropriate to the ground vibrational state has been discussed recently[19] in some detail. Here a brief summary will be given of the results relevant to the current work. Reference 19 will form the ''default option'' for definitions, notation, and mathematical procedures; any changes will be indicated. The internal axis method (IAM) will be used throughout. See Ref. 10.

For the states of low (v_6,J,K) investigated here, the effective Hamiltonian can be written

$$\tilde{H}_g=\tilde{H}_g^{(0)}+\tilde{H}_g^{(1)}, \tag{1}$$

where

$$\tilde{H}_g^{(0)}=B\mathbf{J}^2+(\tilde{A}-B)\mathbf{J}_z^2+\tilde{F}\mathbf{p}^2+\tilde{V}_3\tfrac{1}{2}(1-\cos 3\alpha)+[-D_{Km}\mathbf{p}^2+F_{3K}\tfrac{1}{2}(1-\cos 3\alpha)]\mathbf{J}_z^2, \tag{2}$$

$$\tilde{H}_g^{(1)}=-D_J\mathbf{J}^4-D_{JK}\mathbf{J}^2\mathbf{J}_z^2-D_K\mathbf{J}_z^4-d_J\mathbf{J}_z\mathbf{p}\mathbf{J}^2+[-D_{Jm}\mathbf{p}^2+F_{3J}\tfrac{1}{2}(1-\cos 3\alpha)+F_{6J}\tfrac{1}{2}(1-\cos 6\alpha)]\mathbf{J}^2. \tag{3}$$

In Eqs. (2) and (3), α is the deviation from the equilibrium value of the torsional angle between the methyl top and the silyl frame. $\mathbf{p}$ is traditionally called the torsional angular momentum operator. However, the angular momentum of the internal motion is $\mathbf{p}(1-\rho)$; see Ref. 1. The structural parameter ρ (to the accuracy appropriate to the current work) equals I_α/I_a. Here I_α is the moment of inertia about the symmetry axis of the methyl top and I_a is the corresponding moment for the entire molecule. The reduced rotational constant $\tilde{F}=\tilde{A}/\rho(1-\rho)$.

In Eq. (2), the first two terms form the rigid rotor Hamiltonian $\tilde{H}_R$, while the next two form the zeroth-order torsional Hamiltonian $\tilde{H}_T$. The last two are actually first-order terms that have been moved into zeroth order for computational convenience. These terms provide the leading torsional dependence of the effective A-rotational constant $A^{\mathrm{eff}}(v_6,k,\sigma)$.

In Eq. (3), the first three terms form the usual quartic centrifugal distortion Hamiltonian. The next term is unusual in the sense that it is linear in $\mathbf{J}_z$ and linear in $\mathbf{p}$. The last three terms provide the leading torsional dependence of the effective B-rotational constant $B^{\mathrm{eff}}(v_6,k,\sigma)$. The term in F_{6J} is actually a second-order term (i.e., sextic) that is included in $\tilde{H}_g^{(1)}$ to simplify the notation.

The use of tildes in Eqs. (1) to (3) follows that in a recent work on CH_3CF_3,[20] rather than that in the default option, namely Ref. 19. The tilde on a Hamiltonian term indicates that the form to be used is in the IAM [rather than in the principal axis method (PAM)]. A tilde on a constant indicated an effective value resulting from a transformation or a redundancy.

The separation of the ''tilde-type'' of effective value into the component parts cannot be carried out by frequency measurements on a single isotopomer so long as the contact transformation approach[4,5] does not break down. Such effective values should not be confused with a second type, indicated by the superscript eff, which arises because of limitations in the data set. In this case, the effective parameter is a linear combination of parameters that is useful for breaking correlations in the analysis of a particular data set. However, by such means as using higher resolution and probing a wider range of quantum numbers, the individual contributions can be isolated. These two types of effective values are discussed further in Ref. 21.

The eigenvalues $E_{\mathrm{TR}}(J,v_6,k,\sigma)$ of the torsion–rotation Hamiltonian $\tilde{H}_g$ were calculated by setting up the matrix for $\tilde{H}_g^{(0)}$ in the free-rotor basis, diagonalizing this matrix, and treating $\tilde{H}_g^{(1)}$ by first-order perturbation theory. This is a single-stack approach, the single stack being the set of torsional levels in the ground vibrational state. The perturbations from higher vibrational levels are all nonresonant, and so are absorbed into the effective molecular parameters for the ground-state stack. This procedure is the same as that used in the first stage of the two-stage process described in Sec. II of Ref. 19.

The procedure for determining $E_{\mathrm{TR}}(J,v_6,k,\sigma)$ used in the counterpart paper[11] on CH_3SiH_3 differs from that employed here in two respects. First, the older work included the term $F_{9J}\frac{1}{2}(1-\cos 9\alpha)$ rather than that in F_{6J} in Eq. (3). As discussed in Sec. VI of Ref. 11, it was recognized at that time that this was an unusual step. It was taken because F_{9J} gave a reduction in χ^2 that was significant at the 85% confidence level. However, subsequent works showed that the term in F_{6J} is the better choice when the microwave component of the data set is expanded,[21] and so the F_{6J} choice is made here for CH_3SiD_3 from the beginning.

The second difference is that the terms in D_{Km} and F_{3K} are included here in $\tilde{H}_g^{(0)}$ rather than in $\tilde{H}_g^{(1)}$ as in Ref. 11. This step has the effect of reducing the contribution of the second-order perturbation terms of $\tilde{H}_g^{(1)}$; see Ref. 22. For the low values of J, v_6, and K studied here, this difference is not significant. However, for the large data sets encountered for CH_3SiH_3 (and anticipated for CH_3SiD_3), this reduction is so large[19] that $H_g^{(1)}$ can be treated with first-order perturbation theory, thus simplifying the numerical procedures considerably.

B. Stark energy

The dipole moment matrix elements for a molecule such as CH_3SiD_3 have been discussed previously.[5,6,13,23] Since these matrix elements display some unusual features, a brief review will be given here. Many of the details do not affect the current experiment, but perhaps future work will be stimulated. Matrix elements off diagonal in v_6 provide the transition moment for the torsional bands, but they do not make a significant contribution to the Stark energy and so are not considered. Very recently, the contact transformation approach[4] has been applied to the dipole moment operator for an asymmetric rotor such as methanol by Duan and Takagi.[24] The methods used are very similar to those employed earlier for symmetric rotors such as methyl silane.[5]

Matrix elements diagonal in J are of most interest because the Stark energy $E_S(J,v_6,k,\sigma)$ is dominated by the terms linear in the electric field ξ. For a symmetric rotor with a single torsional degree of freedom, these $(\Delta J=\Delta v_6=0)$ matrix elements can be obtained from their counterparts for a C_{3v} symmetric rotor by replacing the usual dipole constant by an effective dipole moment function. As can be seen from Eq. (4b) of Ref. 6, this can be written

$$\begin{aligned}\mu_Q(J,v_6,k,\sigma)=&\{\tilde{\mu}_0+\mu_0^T\langle\tfrac{1}{2}(1-\cos 3\alpha)\rangle_{v_6,k,\sigma}\\&+\mu_2^T\langle\mathbf{p}^2\rangle_{v_6,k,\sigma}\}+\tilde{\mu}_J^Q J(J+1)+\tilde{\mu}_K k^2\\&+\{\mu_\perp^T J(J+1)+(\tilde{\mu}_\parallel^T-\mu_\perp^T)k^2\}\\&\times\langle\mathbf{p}\rangle_{v_6,k,\sigma}/k.\end{aligned}\tag{4}$$

The angular brackets represent diagonal matrix elements in the basis formed by the eigenfunctions of $\tilde{H}_g^{(0)}$.

The seven independent dipole constants in Eq. (4) are appropriate for characterizing dipole matrix elements calculated in the IAM. Four of these (those labeled with a tilde) have had their physical meaning modified by the PAM-to-IAM transformation. These four are expressed in terms of untransformed parameters in Column I of Table II of Ref. 6. The dipole moment function $\mu_Q(J,v_6,k,\sigma)$ can then be written in terms of seven dipole constants without tildes, the counterparts of the seven in Eq. (4).

The physical meaning of these seven ''untilde'' parameters can be determined by combining the centrifugal distortion work for C_{3v} molecules[25] with the contact transformation analysis for CH_3SiH_3.[5] Except for small corrections, μ_0 is the equilibrium dipole moment, while μ_J^Q and μ_K arise from centrifugal distortion. The remaining four dipole constants (namely those with the superscript T) arise from effects that specifically involve the torsional degree of freedom. Expressions have been derived[5] relating these four parameters to μ_0 and the dipole derivatives. The constant μ_0^T arises in large part from cubic anharmonicity mixing, while μ_2^T is produced entirely from this effect; see Eqs. (27a) and (27b) of Ref. 5. Note that there is a misprint in Eq. (27a); the cubic potential constant K_{66s} should appear as a factor multiplying the sum over the A_1 vibrational modes. Similarly, $\mu_\perp^T$ arises to a significant extent from Coriolis mixing, while $\mu_\parallel^T$ arises entirely from this effect; see Eqs. (4) and (5) of Ref. 23.

For the purposes of the current work, Eq. (4) can be simplified to read

$$\overline{\mu_Q}(J,v_6=0,k)=\mu_{Q,0}^{\mathrm{eff}}+\rho\mu_\perp^T J(J+1)+\rho(\mu_\parallel^T-\mu_\perp^T)k^2.\tag{5}$$

Here the effective dipole moment for the ground torsional state with $J=k=0$ has been written

$$\mu_{Q,0}^{\mathrm{eff}}=\tilde{\mu}_0+\mu_0^T\overline{\langle\tfrac{1}{2}(1-\cos 3\alpha)\rangle_0}+\mu_2^T\overline{\langle\mathbf{p}^2\rangle_0}.\tag{6}$$

Each barred matrix element is the unweighted average over $\sigma=0,+1,-1$ for $v_6=k=0$ of the matrix element of the associated operator. If an alternative value of k is selected to form the average, no significant change occurs.[21] In CH_3SiH_3, $\rho\mu_\perp^T$ and $\rho(\mu_\parallel^T-\mu_\perp^T)$ were found[13] to be 8.83(35) and $-32.87(37)$ μD, respectively, from the (J,k) dependence of $\overline{\mu_Q}(J,0,k)$.

The derivation of Eq. (5) from Eq. (4) is straightforward. *First*, the (k,σ)-dependence of the matrix elements in the terms involving μ_0^T and μ_2^T is not important here. This variation is too small by a factor of four or more in CH_3SiH_3, as can be seen from the discussion in the Appendix of Ref. 13 and the estimates found for μ_0^T and μ_2^T in Ref. 6. *Second*, it

was shown by Jagannath *et al.*[6] that $\tilde{\mu}_J^Q$ and $\tilde{\mu}_K$ could be well approximated by the simplified model defined in Column II of Table II in Ref. 6. That is, these *two constants, which are usually thought of as arising from centrifugal distortion, are largely torsional in origin* in CH_3SiH_3. This simplified model will be adopted here. *Finally*, the term in $\langle \mathbf{p} \rangle_{v_6,k,\sigma}$ can be neglected here. This term is one to two orders of magnitude too small to be significant for CH_3SiH_3, as can be seen from the discussion in the Appendix of Ref. 13 and the values subsequently found for $\mu_\perp^T$ and $(\tilde{\mu}_\parallel^T - \mu_\perp^T)$ in Ref. 6.

In the analysis of the anticrossing data of CH_3SiD_3, it is useful to have an estimate of the J-dependence of $\bar{\mu}_Q$ given in Eq. (5). The estimate obtained here for $\rho\mu_\perp^T$ in CH_3SiD_3 is 6.1 μD. This result can be obtained from Eq. (4) of Ref. 23 and the known value of $\mu_\perp^T$ for CH_3SiH_3 by making *three* simplifying assumptions. *First*, it is assumed for both isotopomers that the centrifugal distortion term involving B_6^{xy} is negligible. *Second*, it is assumed, again for both CH_3SiD_3 and CH_3SiH_3, that the sum over the modes of E_1 symmetry is dominated by the lowest-lying mode of this type, namely the silyl rock with harmonic frequency ω_{12}. Under these assumptions, Eq. (4) of Ref. 23 can be written

$$\mu_\perp^T = 4(4F/9V_3)^{1/4}(B\zeta_{6,12a}^x)(\omega_6\omega_{12})^{1/2} \times (\omega_6^2 - \omega_{12}^2)^{-1}(\partial\mu_x/\partial q_{12a}). \quad (7)$$

Here $\zeta_{6,12a}^x$ is the Coriolis coupling constant between the torsional mode and the silyl rock, while $\partial\mu_x/\partial q_{12a}$ is the derivative of the x-component of the dipole moment with respect to the dimensionless normal coordinate q_{12a}. For each isotopomer, all of the molecular parameters on the right-hand side of Eq. (7) are known (or can be estimated) except the dipole derivative. For CH_3SiH_3, the values are in the literature,[6,7,9] while for CH_3SiD_3 the values are known either from the present work or from a preliminary analysis[26] of ongoing infrared studies.[16] The *third* simplifying assumption is that the dipole derivative is the same for both isotopomers. The ratio of $(\rho\mu_\perp^T)$ for the two molecules [and hence $(\rho\mu_\perp^T)$ for CH_3SiD_3] can then be determined.

For the $(\Delta J = \pm 1)$ matrix elements of the dipole operator, a different dipole moment function, here denoted $\bar{\mu}_R(J, v_6, k)$, must be used; see Eq. (4a) of Ref. 6. This can be simplified in a manner similar to that used for μ_Q. The result can be read from Eq. (5) by setting the term in $J(J+1)$ to zero. This term is omitted because its effect is entirely absorbed into the effective anisotropy $(\alpha_\parallel - \alpha_\perp)_{\text{eff}}$ in the polarizability; see Eq. (5) of Ref. 13.

In calculating the Stark energy $E_S(J, v_6 = 0, k, \sigma)$, the Stark-rotation matrix was diagonalized after truncation at $\Delta J = 3$. In the ''rotational'' terms in this matrix, the effects of internal rotation were neglected. The rotational energies were calculated using effective values for B, D_J, and D_K obtained from lower-state combination differences deduced from a preliminary analysis of the $(v_{12} = 1 \leftarrow 0)$ band.[16] The result of 9622.731 MHz obtained for the effective B-value reproduces the $(v_6 = 0)$ microwave spectrum of Hirota.[15] In the Stark terms in the matrix, $(\alpha_\parallel - \alpha_\perp)_{\text{eff}}$ was held fixed at 1.99×10^{-24} cm^3, the value for CH_3SiH_3.[13] When E_S was being calculated for a particular level (J_r, k_r), the value of $\bar{\mu}_Q$ was set equal to $\bar{\mu}_Q(J_r, 0, k_r)$ for all levels in the matrix. These various approximations are easily shown to be more than adequate for the accuracy required.

III. EXPERIMENTAL DETAILS

The experimental methods and conditions were very similar to those used for CH_3SiH_3.[13,11] The sample was made by reducing CH_3SiCl_3 with $LiAlD_4$. The data were taken using the ion peak with a mass-to-charge ratio of 45. The seeded-beam technique was used; a 5% mixture of methyl silane in argon at a backing pressure between 1 and 1.5 bar was expanded through a 40 μm nozzle with the source at room temperature. The measurements were taken in the earth's magnetic field.

The electric field ξ in the transition region was generated by the Pyrex C-field and stabilization systems developed[27] specifically for large electric fields of high homogeneity. The long-term stability and resettability of the voltage was $\lesssim 20$ ppm. The coating pattern of the plates was as illustrated in Fig. 1 of Ref. 27. For the anticrossing measurements, it was necessary to observe only transitions with $\Delta m_T = 0$, where m_T is the eigenvalue of the component along $\boldsymbol{\xi}$ of the total angular momentum. Consequently, the parallel-plate configuration, which gives better homogeneity, could be used. In this case, the beam direction was as shown in Fig. 1 of Ref. 27, and an interior section with length 3.6 cm along the molecular beam was used. The resulting full width at half maximum of the instrumental line shape due to time of flight was $\Delta\nu_t = 12.5$ kHz. For the electric dipole measurements, $(\Delta m_T = \pm 1)$ transitions had to be studied, and a slit in the C-field parallel to the beam was required.[28] Rather than recoat the Pyrex plates, the C-field was simply rotated through 90°. In this case, the length of the transition region was 10 cm and $\Delta\nu_t = 4.5$ kHz. The fact that the plate separation changed slightly in this step is not relevant.

IV. MEASUREMENTS, ANALYSIS, AND DISCUSSION

A. The dipole moment

The dipole moment $\bar{\mu}_Q(J, v_6 = 0, k)$ was determined for the rotational states $(J,k) = (1,\pm 1)$, $(2,\pm 1)$, and $(3,\pm 2)$ by observing the molecular-beam electric-resonance spectrum in an electric field ξ of 1650.025(80) V/cm. The selection rules obeyed were $\Delta m_J = \pm 1$ and $\Delta J = \Delta k = 0$; in addition, the magnetic quantum numbers for the nuclear spins were conserved. For each (J,K), these transitions between Stark sublevels are denoted $[J_{\pm K}, \mp|m_J| \rightarrow \mp(|m_J| - 1)]$ following the conventions of Ref. 13; see Refs. 10 and 14. Each of the spectra is a multiplet consisting of many hyperfine components, but each appeared as a single line, featureless except for a tail on the high frequency side. A typical signal-to-noise ratio for the $[2_{\pm 1}, \mp 2 \rightarrow \mp 1]$ multiplet, for example, was 20/1; this was obtained with a time constant of 1 s by averaging four sweeps, each of which took 50 s. The central frequency $\nu(J,k,m_J)$ measured for each line is listed in Table I. The electric field was calibrated using the $(J$

TABLE I. Stark measurements and results.[a]

Transition			Frequency $\nu(J,\pm K,m_J)$ (kHz)	Dipole moment (D)	ϵ_R (μD)	ϵ_C (μD)	ϵ_A (μD)
D/H[b]	$J_{\pm K}$	$m_J \rightarrow m_J'$					
D	$1_{\pm 1}$	$\mp 1 \rightarrow 0$	301 915.5 (4.0)	0.725 840	10	17	35
D	$2_{\pm 1}$	$\mp 2 \rightarrow 1$	99 546.2 (4.0)	0.725 885	29	34	45
D	$3_{\pm 2}$	$\mp 2 \rightarrow 1$	100 355.4 (3.0)	0.725 858	22	27	41
H	$3_{\pm 2}$	$\mp 2 \rightarrow 1$	101 568.9 (3.0)	0.734 528	22	27	41
$\bar{\mu}_Q^D(3,0,\pm 2)/\bar{\mu}_Q^H(3,0,\pm 2)$[b]				0.988 197[c]	42[c]		
$\bar{\mu}_Q^D(3,0,\pm 2)/\mu_{\mathrm{OCS}(gs)}$[b,d]				1.014 917[c]		38[c]	

[a]The electric field was 1650.025 V/cm with a relative error of 38 V/cm and an absolute error of 80 V/cm.

[b]The dipole moment function $\bar{\mu}_Q(J,v_6,k)$ is defined in Sec. II A; see Eqs. (4), (5), and (6), in particular. The superscripts D and H refer to CH_3SiD_3 and CH_3SiH_3, respectively.

[c]This is dimensionless.

[d]The subscript gs refers to the ground vibrational state of OCS.

$=1, m_J = \mp 1 \rightarrow 0$) transition of OCS in its ground vibrational state; the OCS Stark parameters used were $\mu = 0.715\,14(3)$ D from Ref. 29 and $(\alpha_\parallel - \alpha_\perp)_{\mathrm{eff}} = 4.67(8) \times 10^{-24}$ cm^3 from Ref. 30.

The observed line shape can be broadened asymmetrically by field inhomogeneities and by nuclear hyperfine interactions. The linewidths from these effects (if each was the sole broadening mechanism) are here denoted $\Delta\nu_\xi$ and $\Delta\nu_{\mathrm{hyp}}$, respectively. The latter is expected to be determined primarily by the quadrupole interaction of the deuterons.

To investigate these widths and shifts, the same three transitions were measured for CH_3SiH_3. All six lines (three for each isotopomer) have roughly the same shape, although the widths varied. For $J_{\pm K} = 3_{\pm 2}$, the quadrupole contribution to the energy vanishes and the line shape (in the absence of inhomogeneities) is symmetric about the hyperfine-free frequency.[31] In this case, the observed linewidth $\Delta\nu_{\mathrm{obs}}$ for each isotopomer was ~ 10 kHz. For CH_3SiD_3, the values of $\Delta\nu_{\mathrm{obs}}$ were 24 and 14 kHz for $J_{\pm K} = 1_{\pm 1}$ and $2_{\pm 1}$, respectively. The corresponding values for CH_3SiH_3 were somewhat smaller. Two conclusions were drawn. First, the field inhomogeneity was ~ 50 ppm. Second, for the $1_{\pm 1}$ and $2_{\pm 1}$ lines, the values of $\Delta\nu_{\mathrm{hyp}}$ were larger by ~ 12 kHz in CH_3SiD_3 than in CH_3SiH_3.

The shifts $\delta\nu_{\mathrm{hyp}}$ of the central frequency away from the hyperfine-free value are of concern, as $\delta\nu_{\mathrm{hyp}}$ will clearly bias the dipole determination. These shifts have been investigated in CH_3CD_3[18] and shown to be $\lesssim 1$ kHz in magnitude. With regard to $\delta\nu_{\mathrm{hyp}}$, the one major difference between these spectra of CH_3CD_3 and CH_3SiD_3 lies in the $1_{\pm 1}$ multiplet. In CH_3CD_3, this multiplet consists of a nearly symmetric triplet with a splitting of about 12 kHz; whereas, for CH_3SiD_3, the much larger value of $\Delta\nu_\xi$ causes these lines to blend into a single feature. However, the asymmetry in the CH_3CD_3 triplet is small enough that, even if these three were blended into a single line, the value of $|\delta\nu_{\mathrm{hyp}}|$ would still be $\lesssim 1$ kHz. It is concluded therefore that $|\delta\nu_{\mathrm{hyp}}|$ in CH_3SiD_3 is also $\lesssim 1$ kHz.

The final experimental uncertainty ϵ assigned to each measurement $\nu(J,k,m_J)$ for CH_3SiD_3 is listed in Table I. In each case, this is estimated from the upper limit on $\delta\nu_{\mathrm{hyp}}$, the signal-to-noise ratio, the linewidth, and the degree of asymmetry in the line shape. Also listed in Table I is the value of $\nu(3,\pm 2,\mp 2)$ measured for CH_3SiH_3.

For each transition, the dipole moment $\bar{\mu}_Q(J,v_6=0,k)$ was determined from the corresponding $\nu(J,k,m_J)$, the OCS transition frequency, and the OCS dipole moment. In each case, the result is given in Table I, along with three different types of error estimates: ϵ_R, ϵ_C, and ϵ_A. The error ϵ_R reflects primarily the uncertainty in the methyl silane frequency; ϵ_R also receives a contribution from the short-term stability of the voltage source, but at 2 ppm this is negligible. ϵ_R is useful in comparing directly the different dipole moments measured for methyl silane. As an example, in Table I, the ratio $\bar{\mu}_Q^D/\bar{\mu}_Q^H$ for the $3_{\pm 2}$ states of CH_3SiD_3 and CH_3SiH_3 is listed. The error ϵ_C includes ϵ_R and the uncertainty in the OCS frequency. ϵ_C is useful in comparing directly the methyl silane dipole moments to the OCS moment. As an example, in Table I, the ratio $\bar{\mu}_Q^D/\mu_{\mathrm{OCS}(gs)}$ for the $3_{\pm 2}$ state of CH_3SiD_3 and the ground vibrational state of OCS is listed. The error ϵ_A includes ϵ_R and the uncertainty of 42 ppm in the OCS dipole moment. ϵ_A is the absolute error.

A check on the current assessment of the asymmetry shifts can be obtained from the value of 1.027 039(38) measured here for the ratio $\bar{\mu}_Q^H/\mu_{\mathrm{OCS}(gs)}$ for the $3_{\pm 2}$ state of CH_3SiH_3 and the ground vibrational state of OCS. In Ref. 13, where the inhomogeneity effects were considerably smaller and a more extensive study was carried out, this ratio was found to be 1.027 057(4), in good agreement with the present result.

In the evaluation of the errors given in Table I for the dipole moments, the long-term stability and resettability of the power supply do not enter because all the frequency measurements (including those for OCS) were taken without altering the voltage setting or disturbing the circuit.

The dipole moment of CH_3SiD_3 has been previously determined by Muenter and Laurie[32] to be 0.7264(20) D using microwave absorption. The value quoted here has been converted to the current best value for $\mu_{\mathrm{OCS}(gs)}$. The agreement with present determination is excellent; see Table I. Furthermore, in Ref. 32, it was found that $\bar{\mu}^D/\bar{\mu}^H = 0.984(4)$, in good agreement with the current value given in Table I.

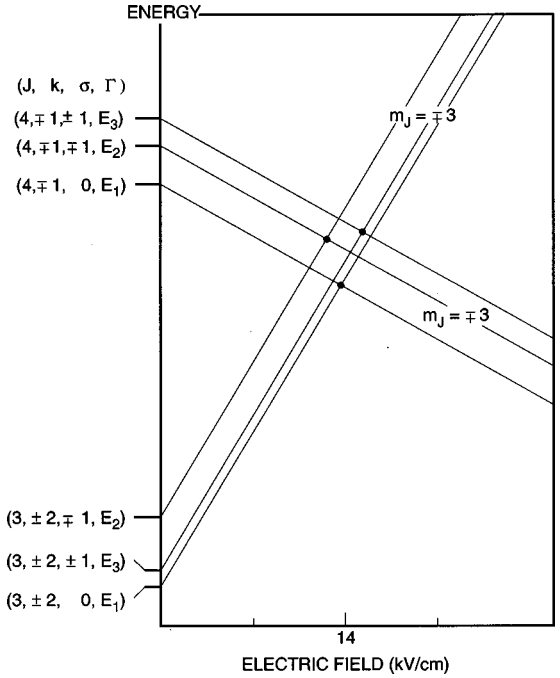

FIG. 1. Schematic plot against the electric field of the energy levels of the states $(J,k)=(4,\mp 1)$ and $(3,\pm 2)$ involved in the rotational anticrossings studied. Upper signs go with upper, and lower with lower. The dots indicate the allowed Stark anticrossings; all were observed. The zero-field σ-splittings are to scale, but are magnified relative to the overall separation of the upper triplet from the lower triplet. As a result, the differences in the crossing fields are exaggerated relative to their average value. The dot for $(\sigma=0)$ corresponds to a zero-field energy difference $\nu^s_{0,0}$ of 3281.6 MHz and a crossing field of 13 906.5 V/cm.

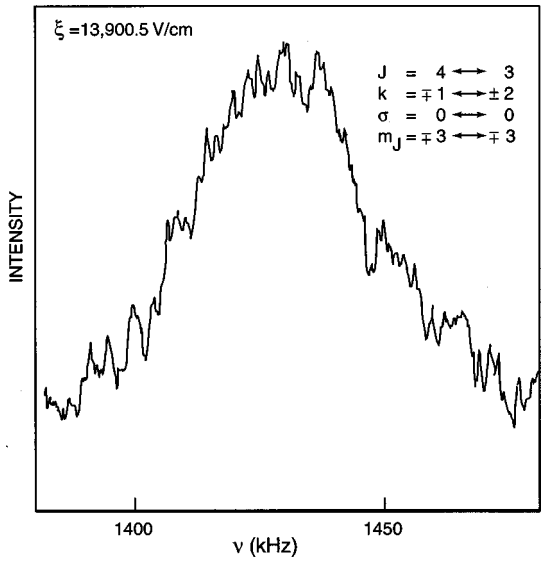

FIG. 2. *Normal* spectrum for a typical rotational anticrossing. The trace was taken 6.1 V/cm below the crossing field. The full width at half height $\Delta\nu_{\rm obs}$ of 42 kHz is determined primarily by field inhomogeneities. Since the difference in Stark energies between the two interacting levels is 3280.1 MHz, the fractional inhomogeneity is ~13 ppm.

B. The torsion–rotation parameters

The set of energy levels probed in the rotational anticrossing study is illustrated in Fig. 1. As an example, consider the two levels with $\sigma=0$, torsion–rotation symmetry $\Gamma=E_1$, and the upper signs.[14] In the limit that the field ξ vanishes, the upper and lower levels are labeled α and β, respectively. In zero field, these levels differ in energy by about 3282 MHz. As the field increases, the upper level with $m_J=-3$ and its lower counterpart approach one another. When the crossing field ξ_c is reached, the difference in the Stark energy E_S for the two levels cancels the corresponding difference in the torsion–rotation energy $E_{\rm TR}$. As the field is increased further, the two levels would cross if there were no interactions between eigenvectors $|\alpha\rangle$ and $|\beta\rangle$. However, they do interact; the levels undergo an avoided crossing. At ξ_c, the levels have their minimum reparation $\nu_{\rm min}$.

For fields near ξ_c, transitions between the interacting levels become allowed and can be detected with electric-resonance molecular-beam methods. A typical spectrum is shown in Fig. 2 for $\sigma=0$. The spectrum is the envelope of all transitions in the multiplet $(4,\mp 1,0,E_1)\leftrightarrow(3,\pm 2,0,E_1)$, including both upper and lower signs as well as all allowed values of the nuclear spin quantum numbers. The trace was obtained with a time constant of 1 s by averaging four sweeps, each of which took 50 s. The measurement was made in a field of 13 900.5(9) V/cm, 6.1 V/cm below the crossing field. This is far enough below ξ_c that the spectrum is *normal*,[33] i.e., the components in the multiplet fall in the same order and with the same separation as they would in the limit $\xi\rightarrow 0$.

The rotational anticrossings studied here are the $(\Delta J=\pm 1)$ counterparts of the $(\Delta J=0)$ Stark rotational anticrossings first observed in CH_3CF_3.[12,34] The mixing between the zero-field eigenstates $|\alpha\rangle$ and $|\beta\rangle$ is provided by the distortion dipole moment μ_D as defined in Ref. 5. The selection rules for the coupling require that the torsion–rotation symmetry Γ be conserved; in addition, σ, m_J, and all the nuclear spin quantum numbers are conserved. For CH_3CF_3, it was possible to measure $\nu_{\rm min}$ and hence μ_D. In the current work, $\nu_{\rm min}$ was too small relative to the observed linewidth $\Delta\nu_{\rm obs}$ of ~45 kHz to be determined. It was shown for $\sigma=0$ that $\nu_{\rm min}\leqslant 40$ kHz and hence that $|\mu_D|\leqslant 1.4$ μD; see Eq. 15 of Ref. 33.

For each anticrossing illustrated in Fig. 1, the zero-field frequency $\nu^s_{\sigma_\alpha\sigma_\beta}$ was determined from the anticrossing data and the calibration procedure outlined in Ref. 27. The experimental uncertainty ϵ was determined following the method given in Ref. 33. The values of $\nu^s_{\sigma_\alpha\sigma_\beta}$ and ϵ are given in Table II. As is shown in the Appendix, the nuclear hyperfine contribution to these frequencies averages to zero in first order. Consequently, the values of ϵ do not have to be adjusted before the $\nu^s_{\sigma_\alpha\sigma_\beta}$ are used in the torsion–rotation analysis. In calculating the difference in Stark energy $(E^\alpha_S-E^\beta_S)$ at the crossing field, the dipole moment $\bar{\mu}_Q(3,0,\pm 2)$ given in Table I was used for state β. For state α, $\bar{\mu}_Q(4,0,\mp 1)$ was calculated by using Eq. (5), the value of $\bar{\mu}_Q(2,0,\mp 1)$ in Table I, and the value of $(\rho\mu_\perp)$ estimated in Sec. II B. The contribution from $(\rho\mu_\perp)$ to each $\nu^s_{\sigma_\alpha\sigma_\beta}$ was only 27 ppm. The values of ϵ given in Table II were calculated assuming that $(\rho\mu_\perp)$ has an uncertainty of 50%. The ''splitting'' method[27] was used to measure the difference $[\nu^s_{0,0}-\nu^s_{\mp 1,\mp 1}]$ directly; the result is also given in Table II. This

TABLE II. Zero-field frequencies[a] in CH_3SiD_3 from anticrossing and microwave experiments.

	Upper state				Lower State				Observed frequency	ϵ[b]	δ[c]	
v_6	J_α	k_α	σ_α	Γ_α	J_β	k_β	σ_β	Γ_β	(MHz)	(KHz)	(kHz)	Label
0	4	∓ 1	0	E_1	3	± 2	0	E_1	3 281.575	165	-16	$\nu^s_{0,0}$
0	4	∓ 1	± 1	E_3	3	± 2	± 1	E_3	3 462.268	175	-9	$\nu^s_{\pm 1,\pm 1}$
0	4	∓ 1	∓ 1	E_2	3	± 2	∓ 1	E_2	3 203.310	165	24	$\nu^s_{\mp 1,\mp 1}$
0				$\nu^s_{0,0}-\nu^s_{\mp 1,\mp 1}$					78.305	8	0	relative
0	1	± 1	∓ 1	E_3	1	∓ 1	0	E_1	212.663	14	0	ν_{EA}
0	2	± 1	∓ 1	E_3	2	∓ 1	0	E_1	212.681	14	0	ν_{EA}
0	1	± 1	∓ 1	E_3	1	∓ 1	∓ 1	E_2	92.415	11	-2	ν_{EE}
0	2	± 1	∓ 1	E_3	2	∓ 1	∓ 1	E_2	92.426	11	2	ν_{EE}
0	1	0	*	*	0	0	*	*	19 245.37[d]	100	-65	$1\leftarrow 0$
1	1	0	*	*	0	0	*	*	19 192.70[d]	100	60	$1\leftarrow 0$
2	1	0	0	A_2	0	0	0	A_1	19 142.84	100	86	$1\leftarrow 0$
2	1	0	± 1	E_4	0	0	± 1	E_4	19 145.41	100	74	$1\leftarrow 0$
0	2	± 1	*	*	1	± 1	*	*	38 490.54[d]	100	33	$2\leftarrow 1$
1	2	± 1	*	*	1	± 1	*	*	38 384.83[d]	100	-30	$2\leftarrow 1$
2	2	± 1	0	E_1	1	± 1	0	E_1	38 285.345	100	-41	$2\leftarrow 1$
2	2	± 1	± 1	E_2	1	± 1	± 1	E_2	38 288.814	100	-25	$2\leftarrow 1$
2	2	± 1	∓ 1	E_3	1	± 1	∓ 1	E_3	38 291.542	100	-14	$2\leftarrow 1$

[a]All transitions are in the ground vibrational state and obey the selection rule $\Delta v_6=0$. The anticrossing measurements are from the current work; the pure rotational frequencies are taken from Ref. 15.

[b]This is the experimental uncertainty. For the pure rotational transitions, no values of ϵ are listed in the original work (Ref. 15). The value of ϵ listed was estimated from the performance of similar instruments in use at the time.

[c]This is the difference between the observed frequency and the value calculated using the parameters in Table III.

[d]This line is an unresolved σ-multiplet. As indicated by the *, the frequency was fit by using the average of the component frequencies, weighted by the relative intensities.

type of relative measurement has the advantage that many of the sources of error are reduced. In this case, ϵ is only 8 kHz instead of ~ 170 kHz, as for the absolute measurements.

The set of energy levels probed for $(J=1)$ in the barrier anticrossing study is illustrated in Fig. 1 of Ref. 18. Although the energy and electric field scales are not appropriate to CH_3SiD_3, the order of the levels is correct and the general form of the diagram is suitable for the current discussion. The two anticrossings labeled with heavy dots were observed. For the dot with the higher crossing field, the zero-field splitting (i.e., frequency) is labeled ν_{EA}, because the upper and lower levels, respectively, have torsional symmetry E and A in zero field. For the dot with the lower crossing field, the zero-field frequency is labeled ν_{EE} for corresponding reasons. The crossing fields are 252.92 and 582.02 V/cm for the EE and EA cases, respectively.

In these barrier anticrossings, the torsion–rotation symmetry Γ changes and $\Delta k=\pm 2$, but all the magnetic quantum numbers are conserved.[11] For the EE case, $(\sigma_\alpha=\mp 1)\leftrightarrow(\sigma_\beta=\mp 1)$, while for the EA case, $(\sigma_\alpha=\mp 1)\leftrightarrow(\sigma_\beta=0)$. For $J=2$, the two corresponding anticrossings were measured: EE, $(J=2,k=\pm 1,\sigma=\mp 1,m_J=\pm 2)\leftrightarrow(2,\mp 1,\mp 1,\pm 2)$; and EA, $(2,\pm 1,\mp 1,\pm 2)\leftrightarrow(2,\mp 1,0,\pm 2)$. The qualitative features of the barrier anticrossing spectra were similar to those of the rotational anticrossings. The observed linewidths $\Delta\nu_{\rm obs}$ were about 45 and 27 kHz for $(J=1)$ and $(J=2)$, respectively.

The matrix element η mixing states α and β is produced by the nuclear hyperfine interactions. In a similar study of CH_3CD_3,[18] it was tentatively concluded that the deuterium quadrupole interaction provides the mixing for the EE anticrossing, while the hydrogen–hydrogen dipolar interaction provides the mixing in the EA case. The latter conclusion is supported by calculations of η for CH_3SiH_3 and CH_3SiF_3.[35] This hyperfine investigation considered the top–top, frame–frame, and top–frame dipolar Hamiltonians. Here these will be denoted as H_{tt}, H_{ff}, and H_{tf}, respectively. The third barrier anticrossing in Fig. 1 of Ref. 18, namely $(1,\pm 1,\pm 1,E_2)\leftrightarrow(1,\mp 1,0,E_1)$, has been shown[35] to derive its mixing matrix element η only from H_{tf}. As this matrix element is very small, no attempt was made to observe this anticrossing for either $(J=1)$ or $(J=2)$.

For each of the four barrier anticrossings observed, the zero-field frequency and its experimental uncertainty were determined using methods similar to those applied to the rotational anticrossings. The results are given in Table II. The dipole moments required were measured directly in the Stark study and are listed in Table I. The $1_{\pm 1}$ value of $\overline{\mu_Q}$ was used for the ν_{EE} and ν_{EA} anticrossings with $(J=1)$; the $2_{\pm 1}$ value of $\overline{\mu_Q}$ was used for the ν_{EE} and ν_{EA} anticrossings with $(J=2)$. For the barrier anticrossings, the nuclear hyperfine interactions can contribute to the zero-field frequencies. The values of the corresponding experimental errors ϵ have been increased so that this contribution can be neglected in the torsion–rotation analysis. For further discussion of the nuclear hyperfine effects, see the Appendix.

In addition to the molecular-beam avoided-crossing measurements, the current data set includes the pure rotational frequencies $\nu_R(v_6,J,k,\sigma)$ measured by Hirota[15] for

TABLE III. Molecular constants for CH_3SiD_3.

Parameter		Value
A^{eff}	(MHz)	34 192.04(11)[a]
B	(MHz)	9 636.606(46)
D_J	(kHz)	7.55[b]
D_{JK}	(kHz)	46.04[b]
D_K	(kHz)	53.27[c]
ρ		0.213 972(23)
V_3^{eff}	(cm^{-1})	585.084(51)[d]
F_{3J}	(MHz)	−115.01(35)
F_{6J}	(MHz)	−5.45(26)
D_{Jm}	(MHz)	0.502(9)
D_{Km}^{eff}	(MHz)	4.44(46)[a]
d_J	(MHz)	−0.095(54)

[a]This effective value is defined by Eq. (16a) or (16b) of Ref. 11. F_{3K} is fixed at zero.
[b]This is fixed at the value obtained in a preliminary analysis of the ($\upsilon_{12}=1\leftarrow 0$) infrared band (Ref. 16).
[c]This is fixed at the force-field value of Ref. 36.
[d]See Eq. (16c) of Ref. 11.

$\upsilon_6 \leqslant 2$; these frequencies are listed in Table II. Hirota's data with $\upsilon_6=3$ and 4 were deliberately omitted. In CH_3SiH_3, it has been shown[9] that a good fit to the pure rotational spectrum of these higher torsional levels cannot be obtained without including the perturbations from the low-lying vibrational states. Furthermore, these perturbations cannot be treated[7] without an extensive data set involving, for example, the ($\upsilon_{12}=1\leftarrow 0$) infrared band. Similar behavior is expected in CH_3SiD_3. For $\upsilon_6=3$ and 4, the differences δ between the observed frequencies and their counterparts calculated from the best fit model (see below) were of the same order in CH_3SiD_3 as they were in CH_3SiH_3 when these perturbations were omitted; see Tables III and IV of Ref. 21.

The data set presented in Table II was analyzed using the methods outlined in Sec. II A; see Eqs. (1) to (3) in particular. In the least-squares fit, D_K was held fixed at its force-field value,[36] while D_J and D_{JK} were held fixed at values determined from combination differences obtained in an infrared study of the ($\upsilon_{12}=1\leftarrow 0$) band.[16] F_{3K} was fixed at zero, and the effective values A^{eff} and D_{Km}^{eff} were introduced as defined, respectively, in Eqs. (16a) and (16b) of Ref. 11. $\tilde{F}$ was calculated from $\tilde{A}^{\text{eff}}$ and ρ, with ρ replacing $\tilde{F}$ as an independent parameter. By varying the eight remaining parameters in Eqs. (2) and (3), as well as ρ, a good fit was obtained. The best-fit values of the molecular parameters are listed in Table III. The difference δ between each observed frequency and its counterpart calculated with these best fit values is given in Table II.

The results obtained here for the molecular parameters are substantially more accurate than those obtained earlier[15] using the Kivelson satellite method[37] for reasons mentioned in Sec. I and discussed in more detail in Sec. I of Ref. 20. Moreover, the present results represent the data very well. However, as the data set is expanded, some of the effective values can be expected to change by many times the statistical errors given in Table III. For example, the value of V_3^{eff} obtained in Ref. 11 for CH_3SiH_3 from a data set comparable to that used here is 0.925 cm^{-1} larger than the value of $\tilde{V}_3$ obtained in Ref. 9 from a two-band analysis involving over 2700 frequencies.

Nonetheless, it is instructive to compare the present CH_3SiD_3 results with their CH_3SiH_3 counterparts[11] obtained from a data set of similar scope by using a similar Hamiltonian model; see Table III here and Table IV in Ref. 11. The value of V_3^{eff} is smaller in CH_3SiD_3 by 7.26 cm^{-1}, a difference which is likely to remain approximately constant (at least to 1 cm^{-1} or so) as the CH_3SiD_3 data set expands. The barrier height is also reduced in ethane when the frame is fully deuterated. The barrier heights in CH_3CD_3[23] and CH_3CH_3[38] are 993.8 and 1012.5 cm^{-1}, respectively. The fact that the barrier height is lowered upon deuteration is perhaps not a surprise. The amplitude of the zero-point motion of the deuterium atoms is smaller and the CD bond length is shorter than the CH bond length. However, an in-depth discussion of these effects must wait until the contribution to the effective barrier height from rotation–vibration interactions is better understood.

It should also be noted that each torsional distortion constant in CH_3SiD_3 has the same sign as its counterpart in CH_3SiH_3 and is smaller in magnitude by a factor of 1.2 to 2.4. This general behavior is expected in general when the frame becomes heavier.

V. CONCLUSION

The first phase has been completed of a study of the changes in the vibration–torsion–rotation and electric-dipole constants of methyl silane when the silyl frame is fully deuterated. Once the torsional bands and the low-lying vibrational fundamentals have been investigated and the pure rotational spectrum has been measured in the mm-wave region, it should be possible to obtain a greater understanding of the different physical mechanisms that underlie these molecular parameters.

ACKNOWLEDGMENTS

The authors wish to thank Mr. J. Schroderus for many fruitful discussions. One of us (I.O.) wishes to express his appreciation to the Natural Sciences and Engineering Research Council of Canada for partial funding of this research. I.O. is particularly grateful to the University of Nijmegen for its financial support while this manuscript was being prepared.

APPENDIX: HYPERFINE SHIFTS FOR CH_3SiD_3, CH_3SiH_3, CH_3SiF_3, AND CH_3CD_3

The possibility of a hyperfine shift $\delta\nu_{\text{hyp}}$ in the zero-field frequencies obtained in these anticrossing experiments is of particular concern in the current work, because the deuterium quadrupole Hamiltonian, here denoted H_Q^D, can be expected to produce larger effects than the spin–rotation and spin–spin interactions. Consider a *normal* spectrum (as defined in Sec. IV B); Fig. 2 provides an example. To synthesize this envelope, first a stick spectrum would be constructed for the individual hyperfine components by assigning to the ith such component its intensity Y_i and hyperfine shift $\delta\nu_i$ away from the hyperfine-free frequency ν_0. Then the stick spectrum

would be convolved with the effective instrumental line shape of linewidth $\Delta\nu_{\text{eff}}$. The problem then is to estimate the difference $\delta\nu_{\text{hyp}}$ between the measured central frequency for the resulting envelope and the hyperfine-free value ν_0.

Unfortunately, the form of H_Q^D for a molecule of the symmetry of CH_3SiD_3 has not been developed. However, the corresponding operator for CH_3D[39] can be used to deduce the qualitative features of the spectrum and to estimate $\delta\nu_{\text{hyp}}$. The deuterium quadrupole coupling constant eqQ will be taken to be 200 kHz. [In CH_3CD_3, it is (167 $\pm$18) kHz.[40]]

Consider the Stark rotational anticrossings first. In the lower state β, the diagonal matrix elements $\langle H_Q^D\rangle_i$ equal zero for all i since each matrix element will contain the factor $[3K^2-J(J+1)]$, which vanishes for $J_{\pm K}=3_{\pm 2}$. Thus $\delta\nu_i$ is simply $\langle H_Q^D\rangle_i$ for the upper state α with $J=4$ and $k=\mp 1$. It is easily shown that the shifts $\delta\nu_i$ are asymmetrically distributed, but that the average value vanishes. Because the mixing between states α and β due to the distortion dipole moment is independent of the nuclear spin quantum numbers, the transition moment is independent of i [see Eq. (12) of Ref. 33], and all Y_i are equal. It follows then that the center of gravity of the distribution falls at the hyperfine-free value ν_0. If $\Delta\nu_{\text{eff}}\gtrsim$ the frequency difference $\Delta\nu_{\max}$ between the highest and lowest frequency hyperfine components, the resulting envelope will be asymmetric to some degree, but the central frequency will not be shifted significantly.

In the current work, the splitting $\Delta\nu_{\max}$ due to eqQ in the Stark rotational anticrossing spectra observed is estimated to be 12 kHz, which is almost a factor of four smaller then the observed linewidth $\Delta\nu_{\text{obs}}$ of $\sim$45 kHz. Thus $\delta\nu_{\text{hyp}}$ should be negligible compared with the experimental uncertainty ϵ of 8 kHz in the relative measurement listed in Table II.

Now consider the barrier anticrossings. It was *stated* in Ref. 11 that the states α and β differ only in the sign of k and, for the EA anticrossing, in σ. It was then *concluded* that, except possibly for small σ-dependent terms, states α and β have the same diagonal hyperfine matrix elements and $\delta\nu_{\text{hyp}}$ is consequently zero. This statement and conclusion are incorrect. The states α and β also differ in the torsion–rotation symmetry Γ. Moreover, α and β differ in the total spin I_t for the three identical top nuclei and/or the total spin I_f for the three identical frame nuclei. The diagonal quadrupole matrix elements $\langle H_D^Q\rangle_i$ will depend on I_f, as can be seen from Table IV of Ref. 39. As a result, the individual $\delta\nu_i$ can be nonzero.

Furthermore, it is possible for a hyperfine interaction to be forbidden in state α, for example, and allowed in state β. An example of just such a case exists for CH_3SiH_3. For $I_t=1/2$, the diagonal matrix elements $\langle H_{tt}\rangle_i$ of the top–top spin–spin interaction[41] vanish because H_{tt} is a second rank tensor in I_t.[42] On the other hand, $\langle H_{tt}\rangle_i$ does not vanish if $I_t=3/2$. Similar statements apply to H_{ff}, but not to H_{tf}.[41] From Table XIII of Ref. 35, it is then easily seen that $\langle H_{tt}\rangle_i$ vanishes for $\Gamma=E_3$, but not for $\Gamma=E_1$. Thus $\langle H_{tt}\rangle_i$ will make a direct contribution to $\delta\nu_i$ for the EA anticrossings [in which $(\Gamma_\alpha=E_3)\leftrightarrow(\Gamma_\beta=E_1)$]. $\langle H_{ff}\rangle_i$ plays a similar role in the EE anticrossings.

Although $\delta\nu_i$ can be nonzero, in general, it might still follow that $\delta\nu_{\text{hyp}}=0$, as was the case for the rotational anticrossings previously considered. However, for the barrier anticrossings, the mixing between states α and β arises from the hyperfine Hamiltonian. Consequently, the transition moment and the intensity Y_i will depend on i (i.e., on the nuclear spin quantum numbers). Furthermore, since I_t and/or I_f changes, some particular i may be excluded by the selection rules. In general, then, the center of gravity will not fall at the hyperfine-free frequency ν_0 and $\delta\nu_{\text{hyp}}\neq 0$.

In the current work on CH_3SiD_3, the value of $\delta\nu_{\text{hyp}}$ is estimated conservatively as one-half of the maximum shift possible from the diagonal quadrupole matrix elements $\langle H_Q^D\rangle_i$. This estimate for the magnitude of $\delta\nu_{\text{hyp}}$ is 5 kHz for $J=1$ and 7 kHz for $J=2$. The errors ϵ given in Table II have been increased to allow for these estimates of $|\delta\nu_{\text{hyp}}|$. The increase is not serious since the uncertainties from other sources are $\gtrsim|\delta\nu_{\text{hyp}}|$. The contributions to $\delta\nu_{\text{hyp}}$ from the spin–rotation and spin–spin interactions (see below) were estimated and found to be smaller than the quadrupolar contribution.

In earlier studies of barrier anticrossings in CH_3SiH_3,[11] CH_3SiF_3,[17] and CH_3CD_3,[18] $\delta\nu_{\text{hyp}}$ was neglected on the basis of the Ref. 11 argument. The contribution of $\delta\nu_{\text{hyp}}$ to the frequencies measured in these earlier studies has now been reevaluated.

For CH_3SiH_3, $\delta\nu_{\text{hyp}}$ can be estimated by adapting the energy expression for the fluorine spin–rotation and fluorine–fluorine dipolar interactions in OPF_3; see Eq. (2) of Ref. 31. For each state α and β in the barrier anticrossing, the values of I_t and I_f were taken from Table XIII of Ref. 35. The direct spin–spin coupling constant can be calculated from the structure.[21] From the known spin–rotation constants for CH_4[43] and SiH_4,[44] the spin-rotation constants for $\mathbf{I}_t$ and $\mathbf{I}_f$, respectively, in CH_3SiH_3 can be estimated by assuming that these coupling constants are proportional to their associated rotational constants.

The spin–spin contributions to $\delta\nu_i$ are of the same order as the spin–rotation contributions from the terms in $(c_\parallel^t-c_\perp^t)$ and $(c_\parallel^f-c_\perp^f)$. The superscripts t and f, respectively, refer to top and frame spin–rotation interactions. The subscripts $\parallel$ and $\perp$, respectively, refer to the z and x diagonal elements of the spin–rotation tensor. The spin–spin contributions increase with J, while the spin–rotation contributions decrease with J; the overall value of $\delta\nu_{\text{hyp}}$ can be taken to be roughly independent of J. The estimated values for $|\delta\nu_{\text{hyp}}|$ are 4 and 6 kHz, respectively, for the EE and EA anticrossings. These values of $|\delta\nu_{\text{hyp}}|$ should be added in quadrature to the errors listed in the original work; see Table II of Ref. 11. The resulting increases in these errors are small because each original error is larger in magnitude than its associated value of $|\delta\nu_{\text{hyp}}|$. The effect on the published values of the molecular parameters for CH_3SiH_3[9] is negligible.

A similar analysis was carried out in CH_3SiF_3. In this case, the spin–rotation constants for the frame were estimated using the information available on the spin–rotation tensor of SiF_4.[45,46] As was the case with CH_3SiH_3, the spin–spin and spin–rotation contributions to the $\delta\nu_i$ in CH_3SiF_3 were of the same order, but for this molecule the leading spin–rotation contribution arose from the term in $c_\perp^f$. The

estimated values for $|\delta\nu_{\rm hyp}|$ are 2 kHz for the EE anticrossings, 3 kHz for the EA avoided crossings for $J\leqslant 3$, and 6 kHz for the EA anticrossing for $J=5$ (as well as for the relative EA measurement involving $J=5$ and $J=2$). The $(J=5)$ value of $|\delta\nu_{\rm hyp}|$ is larger because this particular anticrossing was measured for $m_J=\pm 5$, whereas all the other measurements were for $m_J=\pm 1$. These values of $|\delta\nu_{\rm hyp}|$ should be added in quadrature to the original errors listed in the original work; see Table 3 of Ref. 17. For CH_3SiF_3, the contribution to the final error estimates from $\delta\nu_{\rm hyp}$ is dominant for each of the last three entries in Table 3 of Ref. 17. For each of these measurements, $|\delta\nu_{\rm hyp}|$ is a factor of five larger than the original error estimate, which was ~ 1 kHz. The effect of the increase in the error estimates on the torsion–rotation parameters obtained is expected to be small; this effect will be discussed elsewhere.[47]

For CH_3CD_3, the analysis is essentially the same as that for CH_3SiD_3. The estimates for $|\delta\nu_{\rm hyp}|$ as one-half of the maximum shift due to H_Q^D are 5 and 7 kHz, respectively, for $J=1$ and 2. In this case, $\delta\nu_{\rm hyp}$ dominates the final error estimates because the errors from other sources are ~ 1 kHz. This contribution from $\delta\nu_{\rm hyp}$ may explain the inconsistency pointed out[48] between the anticrossing data and the mm-wave spectrum. It was suggested that systematic effects in the beam measurements of ~ 5 kHz would account for the disagreement. The increase in these error limits has only marginal effects on the results published recently[49] on the infrared band $(\upsilon_{12}=1\leftarrow 0)$ of CH_3CD_3.

[1] C. C. Lin and J. D. Swalen, Rev. Mod. Phys. **31**, 841 (1959).
[2] W. Gordy and R. L. Cook, *Microwave Molecular Spectra*, 3rd ed. (Wiley, New York, 1984).
[3] R. M. Lees and J. G. Baker, J. Chem. Phys. **48**, 5299 (1968).
[4] D. Papousek and M. R. Aliev, *Molecular Vibrational-Rotational Spectra* (Elsevier, Amsterdam, 1982).
[5] N. Moazzen-Ahmadi and I. Ozier, J. Mol. Spectrosc. **126**, 99 (1987).
[6] H. Jagannath, I. Ozier, and N. Moazzen-Ahmadi, J. Mol. Spectrosc. **119**, 313 (1986).
[7] N. Moazzen-Ahmadi, I. Ozier, and W. L. Meerts, J. Mol. Spectrosc. **137**, 166 (1989).
[8] J. Susskind, D. Reuter, D. E. Jennings, S. J. Daunt, W. E. Blass, and G. W. Halsey, J. Chem. Phys. **77**, 2728 (1982).
[9] N. Moazzen-Ahmadi, I. Ozier, G. A. McRae, and E. A. Cohen, J. Mol. Spectrosc. **175**, 54 (1996).
[10] In the current work, k represents the eigenvalue of the component of **J** along the molecular symmetry axis $\hat{z}$, while $K\equiv|k|$.
[11] W. L. Meerts and I. Ozier, J. Mol. Spectrosc. **94**, 38 (1982).
[12] W. L. Meerts and I. Ozier, Phys. Rev. Lett. **41**, 1109 (1978).
[13] I. Ozier and W. L. Meerts, J. Mol. Spectrosc. **93**, 164 (1982).
[14] It is understood in the current work that upper signs go with upper, and lower with lower.
[15] E. Hirota, J. Mol. Spectrosc. **43**, 36 (1972).
[16] J. Schroderus, I. Ozier, W. Ho, and N. Moazzen-Ahmadi (private communication).
[17] W. L. Meerts and I. Ozier, Chem. Phys. **71**, 401 (1982).
[18] I. Ozier and W. L. Meerts, Can. J. Phys. **62**, 1844 (1984); **63**, 1375 (1985).
[19] N. Moazzen-Ahmadi, I. Ozier, E. H. Wishnow, and H. P. Gush, J. Mol. Spectrosc. **170**, 516 (1995).
[20] I. Ozier, J. Schroderus, S.-X. Wang, G. A. McRae, M. C. L. Gerry, B. Vogelsanger, and A. Bauder, J. Mol. Spectrosc. **190**, 324 (1998).
[21] M. Wong, I. Ozier, and W. L. Meerts, J. Mol. Spectrosc. **102**, 89 (1983).
[22] N. Moazzen-Ahmadi, I. Ozier, and H. Jagannath, J. Mol. Spectrosc. **119**, 299 (1986).
[23] N. Moazzen-Ahmadi, I. Ozier, A. R. W. McKellar, and F. Zerbetto, J. Chem. Phys. **105**, 8536 (1996).
[24] Y.-B. Duan and K. Takagi, J. Chem. Phys. **104**, 7395 (1996).
[25] J. K. G. Watson, M. Takami, and T. Oka, J. Chem. Phys. **70**, 5376 (1979).
[26] To good approximation, the unpublished information can be replaced by the approximate value of ω_{12} in J. L. Duncan, A. M. Ferguson, and D. C. McKean, J. Mol. Spectrosc. **168**, 522 (1994), and estimates made using the CH_3SiH_3 values.
[27] W. L. Meerts and I. Ozier, J. Chem. Phys. **75**, 596 (1981).
[28] T. C. English and J. C. Zorn, in *Methods of Experimental Physics*, edited by Dudley Williams (Academic, New York, 1974), Vol. 3, Part B.
[29] J. M. L. J. Reinartz and A. Dymanus, Chem. Phys. Lett. **24**, 346 (1974).
[30] L. H. Scharpen, J. S. Muenter, and V. W. Laurie, J. Chem. Phys. **53**, 2513 (1970).
[31] W. L. Meerts, I. Ozier, and A. Dymanus, Can. J. Phys. **57**, 1163 (1979).
[32] J. S. Muenter and V. W. Laurie, J. Chem. Phys. **45**, 855 (1966).
[33] I. Ozier and W. L. Meerts, Can. J. Phys. **59**, 150 (1981).
[34] W. L. Meerts and I. Ozier, Chem. Phys. **152**, 241 (1991).
[35] J. T. Hougen, W. L. Meerts, and I. Ozier, J. Mol. Spectrosc. **146**, 8 (1991).
[36] E. A. Clark and A. Weber, J. Chem. Phys. **45**, 1759 (1966).
[37] D. Kivelson, J. Chem. Phys. **22**, 1733 (1954).
[38] N. Moazzen-Ahmadi, A. R. W. McKellar, J. W. C. Johns, and I. Ozier, J. Chem. Phys. **97**, 3981 (1992).
[39] S. C. Wofsy, J. S. Muenter, and W. Klemperer, J. Chem. Phys. **53**, 4005 (1970).
[40] F. S. Millett and B. P. Dailey, J. Chem. Phys. **56**, 3249 (1972).
[41] H_{tt}, H_{ff}, and H_{tf} were introduced in Sec. IV B.
[42] A. R. Edmonds, *Angular Momentum in Quantum Mechanics* (Princeton University Press, Princeton, NJ, 1974).
[43] W. M. Itano and I. Ozier, J. Chem. Phys. **72**, 3700 (1980).
[44] W. M. Itano and N. F. Ramsey, J. Chem. Phys. **72**, 4941 (1980).
[45] I. Ozier, S. S. Lee, and N. F. Ramsey, J. Chem. Phys. **65**, 3985 (1976).
[46] I. Ozier, L. M. Crapo, and S. S. Lee, Phys. Rev. **172**, 63 (1968).
[47] C. Styger, I. Ozier, J. Schroderus, and A. Bauder (private communication).
[48] N. Moazzen-Ahmadi, I. Ozier, I. Mukhopadhyay, and T. Amano, J. Chem. Phys. **99**, 2429 (1993).
[49] N. Moazzen-Ahmadi, I. Ozier, I. Mukhopadhyay, and A. R. W. McKellar, J. Chem. Phys. **108**, 838 (1998).